	Radiochemical purity (%)	Specific activity (Ci/g)
^{225}Ac-E4G10	97.6 ± 2.4	0.19 ± 0.1
^{225}Ac-Isotype	98.7 ± 0.84	0.13 ± 0.08

Supplemental Table 1. Radiolabeling statistics for the ^{225}Ac labeling of the specific antibody E4G10 and the isotype control antibody for in vivo studies. Statistics are displayed for n = 16 labelings for E4G10 and *n* = 10 for the isotype control antibody.

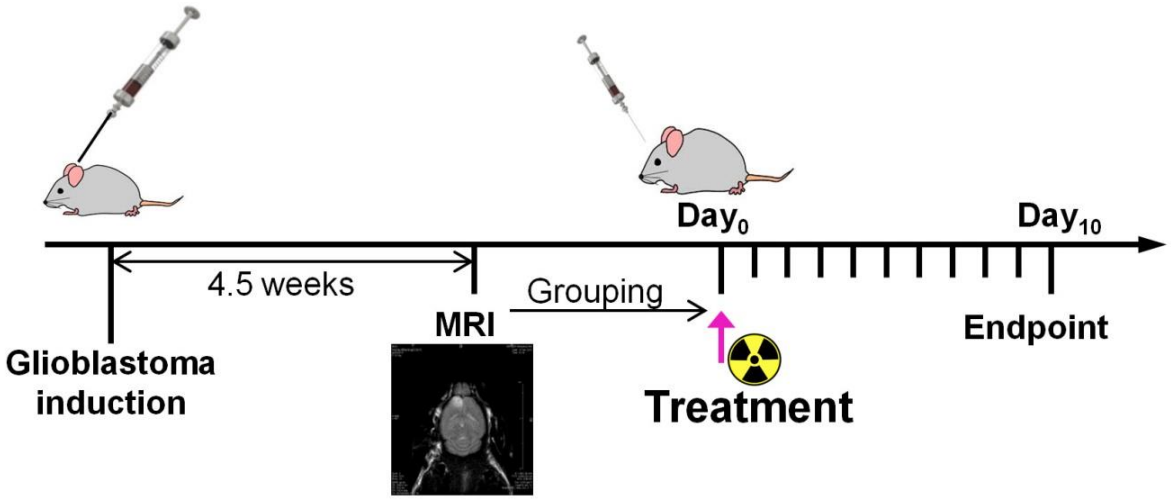

Supplemental Figure 1. Experimental setup for mechanistic in vivo studies of ^{225}Ac-E4G10-treatment in Ntva-tumor model. At the age of 4–10 weeks, Ntva-mice were induced with glioblastoma tumor by stereotactic gene delivery of hPDGF to nestin-driven stem cells in the brain. Mice were screened for tumor growth and tumor size 4.5 weeks after tumor induction with T2 MR imaging and grouped into treatment groups with an even distribution of tumor sizes. Treatment with ^{225}Ac-E4G10 or ^{225}Ac-isotype control was administered as a single dose of 200 nCi at day 0. Mice were sacrificed and tissues analyzed ten days after the treatment.

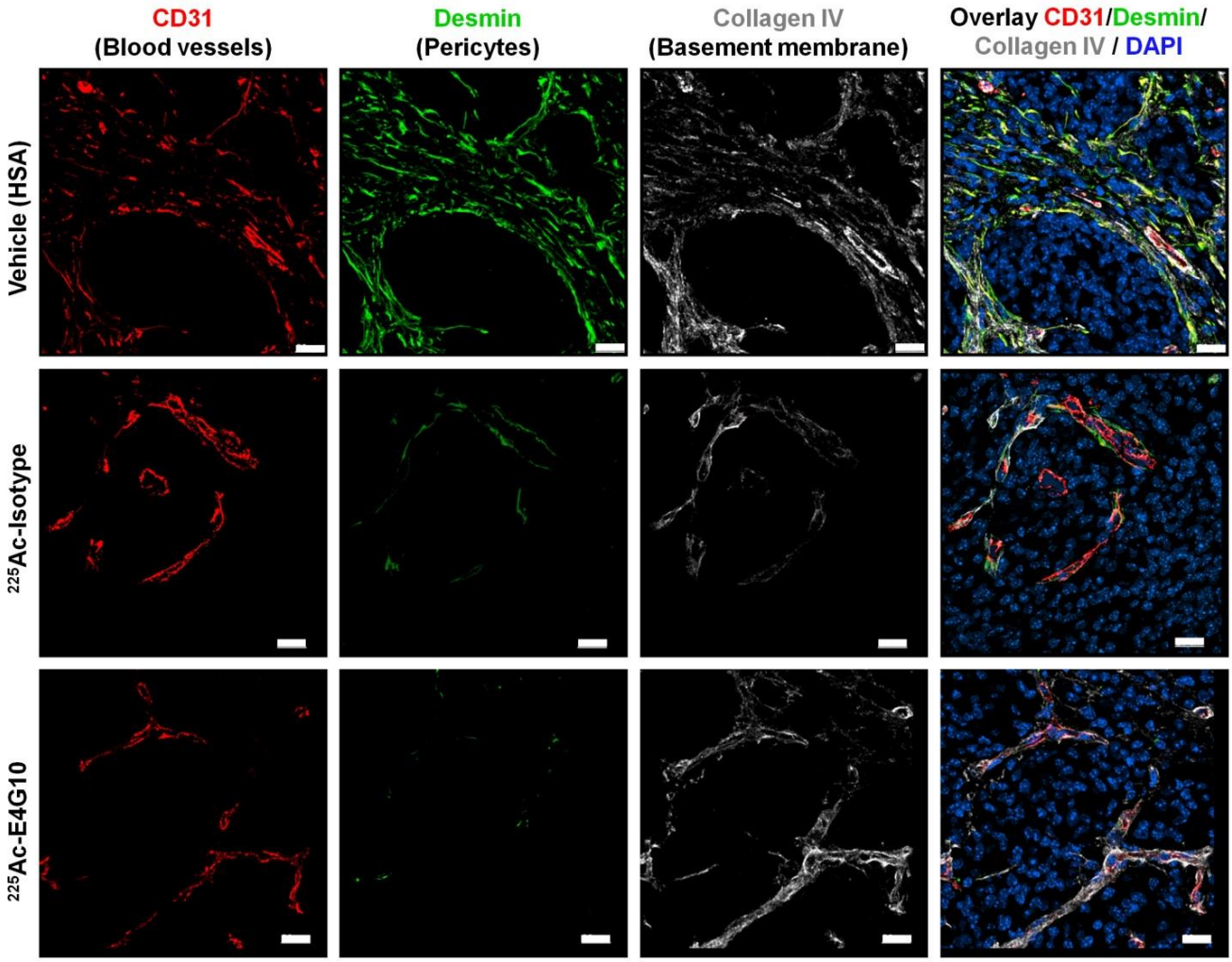

Supplemental Figure 2. Confocal immunofluorescence (IF) imaging of tumor sections costained for anti-CD31 for endothelial cells, anti-Desmin for perivascular cells and anti-CollagenIV for basement membrane. The last row shows the overlay from Figure 1A of all stains with colocalization of endothelial cells (red) and pericytes (green) shown in yellow and nuclear counterstaining with DAPI (blue). Scale bars are 20 µm.

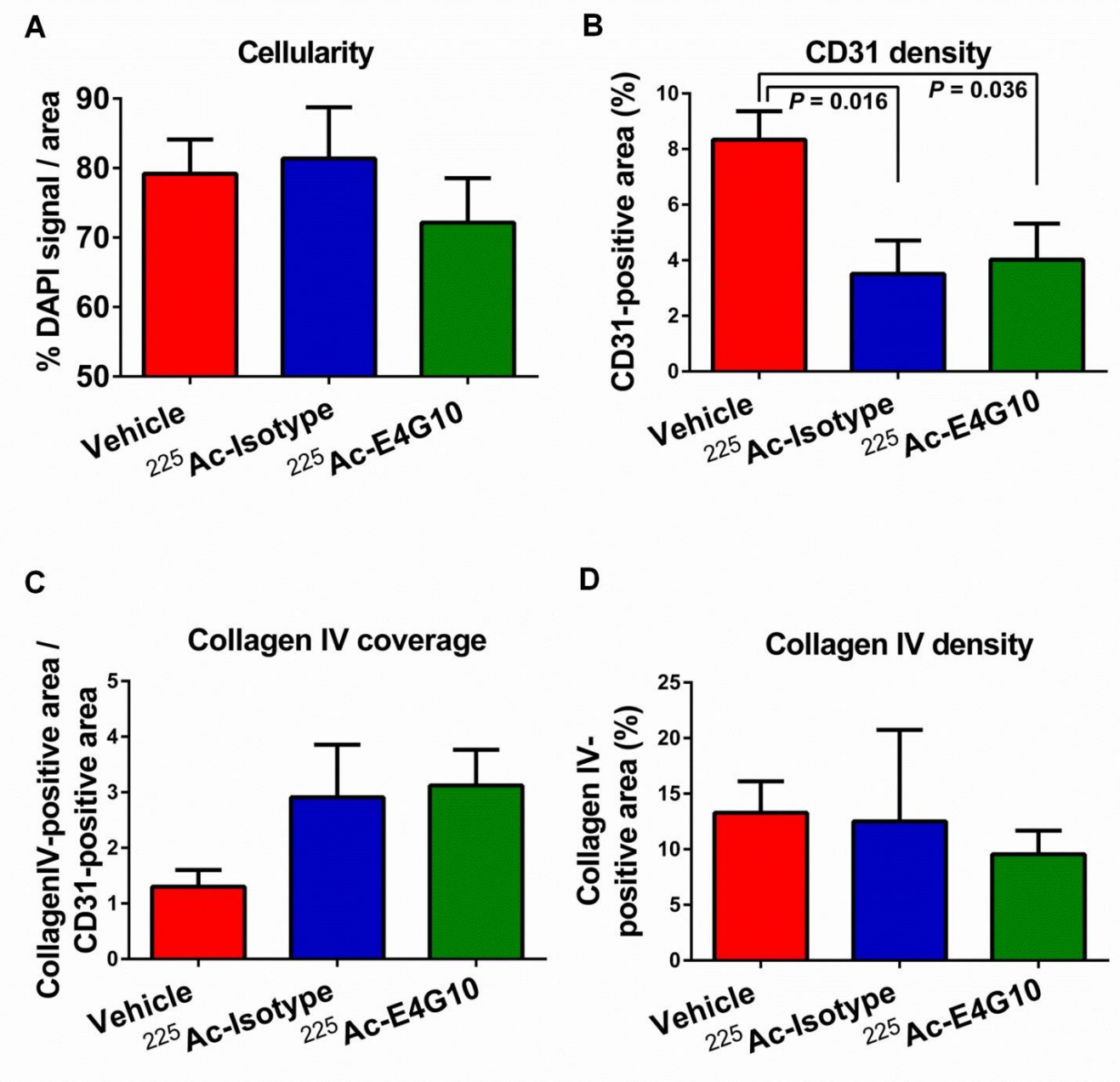

Supplemental Figure 3. Quantification of IF images of whole tumor sections of treated glioblastomas stained for CD31, Desmin, CollagenIV, and DAPI (n = 4 for every treatment group). Values are mean ± SEM. (**A**) Cellularity. (**B**) EC density (CD31 normalized by DAPI). (**C**) CollagenIV coverage (CollagenIV normalized by CD31). (**D**) CollagenIV density (CollagenIV normalized by DAPI).

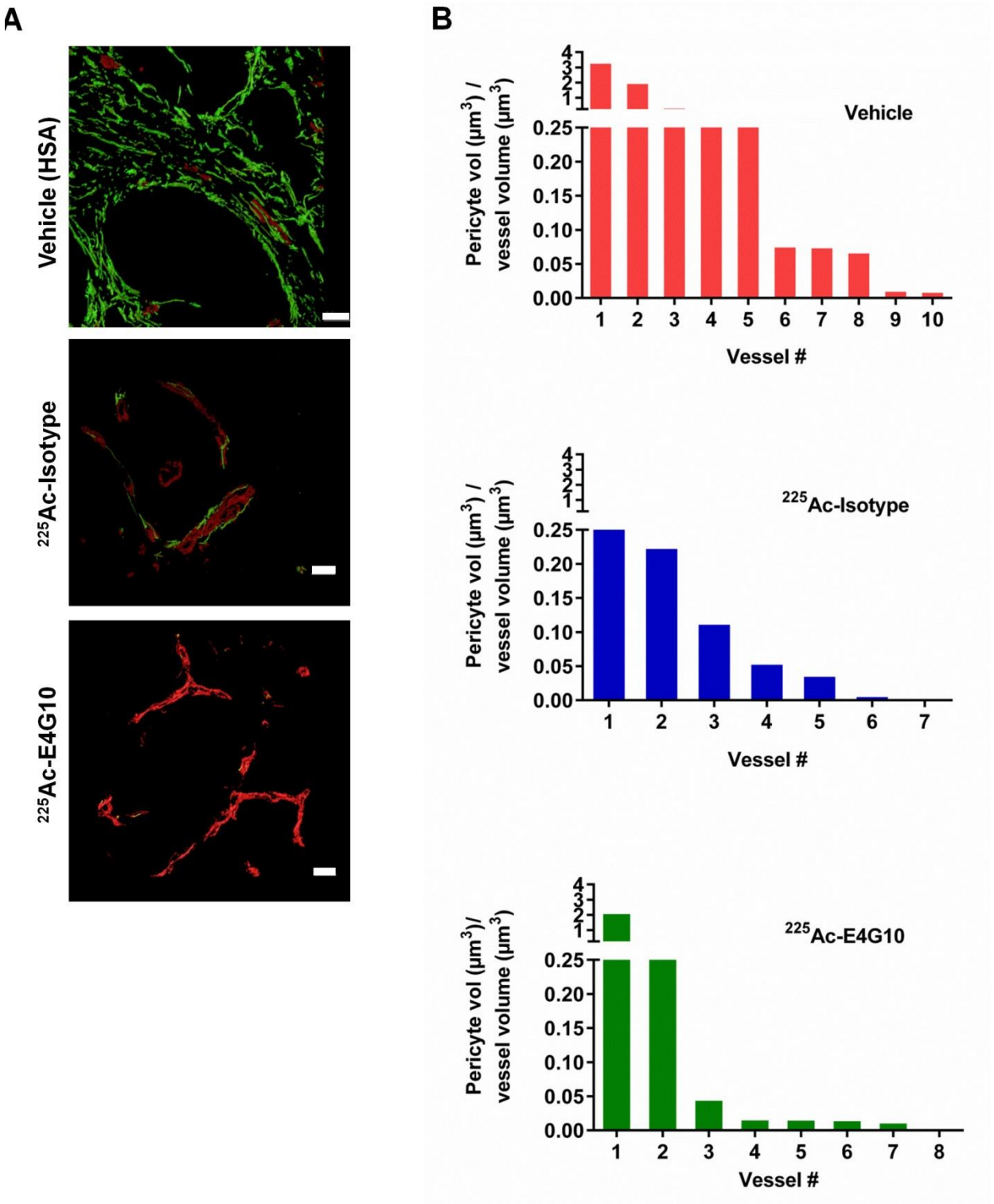

Supplemental Figure 4. (**A**) 3D projection of confocal IF images of tumor sections stained for blood vessels and pericytes. Scale bars are 20 µm. (**B**) Quantification of pericyte association of individual blood vessels. ^{225}Ac-E4G10–treated individual vessels show less pericyte coverage than vehicle-treated vessels. 75% of all investigated ^{225}Ac-E4G10–treated vessel units were found to be covered by pericytes below 5%, compared with 20% of vessels in the vehicle-treated group. Reconstructed z-stacks of confocal IF images were used to determine the ratio of pericyte volume to associated vessel volume. Note that individual vessels with no pericyte coverage (as found in reconstructed z-stacks of ^{225}Ac-E4G10–treated samples) were not included in the graph.

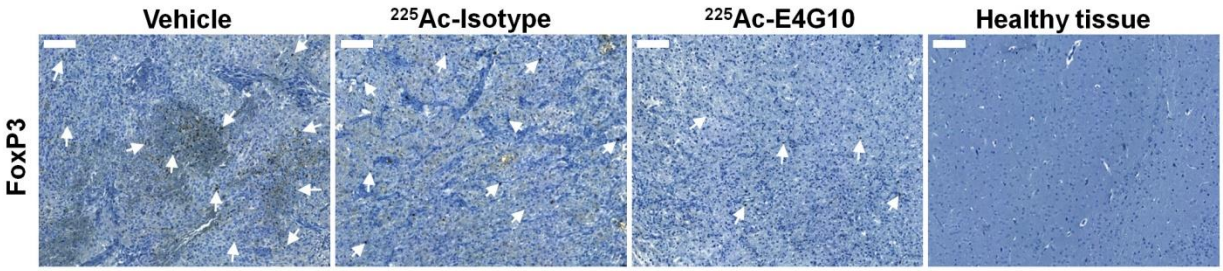

Supplemental Figure 5. FoxP3 immunohistochemical staining for the identification of regulatory T cells. Shown are representative sections from treated glioblastoma tumors (n = 4 in every treatment group) stained with anti-FoxP3 antibody, as shown in Figure 1D compared with ^{225}Ac-isotype–treated and healthy tissue samples. The FoxP3 signal was absent from healthy brain. Arrows indicate FoxP3^{+} cells. Scale bars are 100 μm.

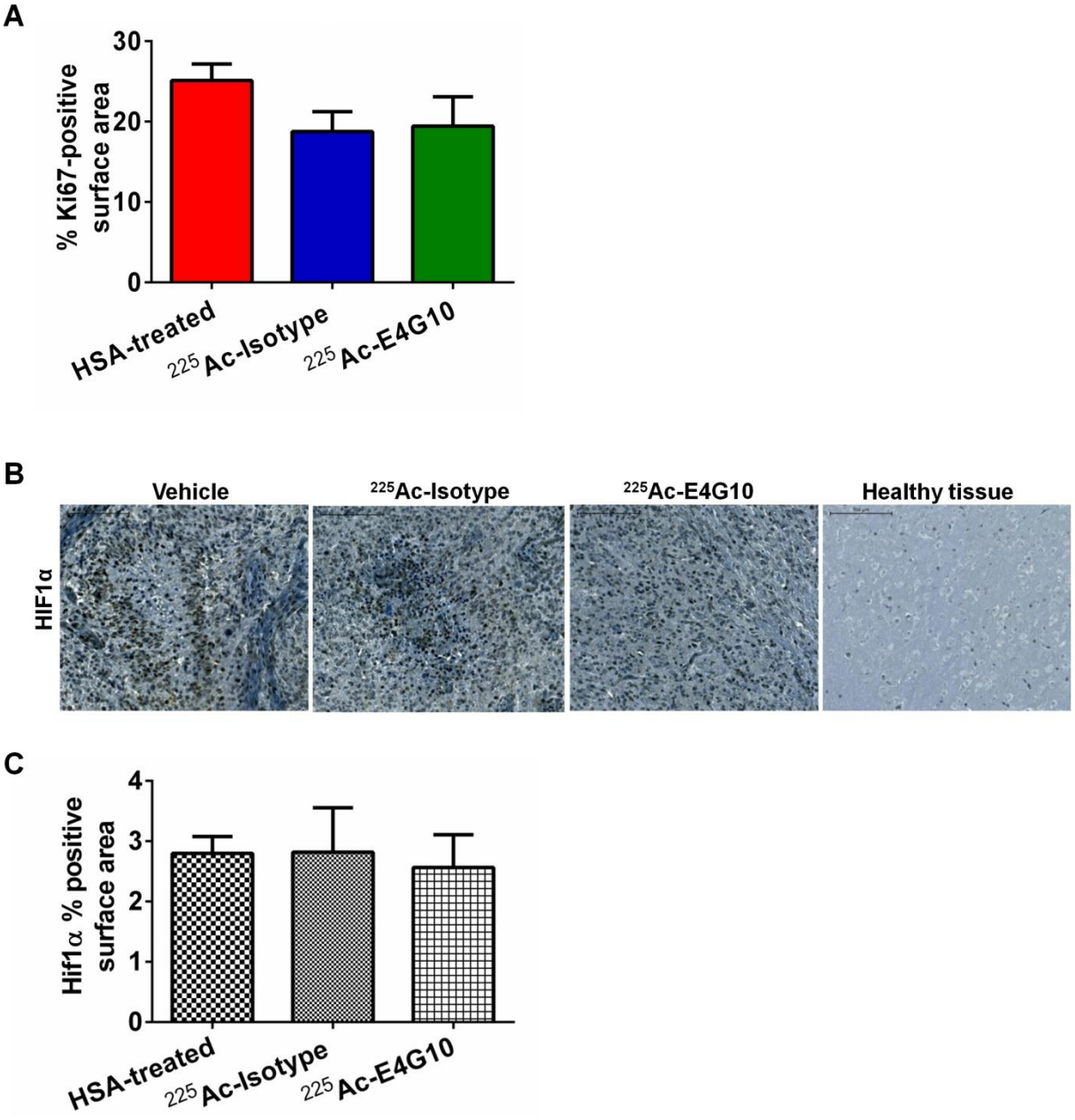

Supplemental Figure 6. Proliferation (**A**) and hypoxia (**B**) in ^{225}Ac-E4G10–treated glioblastoma tumor sections. ^{225}Ac-E4G10–treated tumors show a trend toward decreased proliferation and hypoxia compared with vehicle-treated controls, without reaching statistical significance. Proliferating cells were stained with anti-Ki67 antibody, and hypoxia was assessed using an anti-HIF1α antibody. IHC images show representative samples of every treatment group (n = 4). Scale bars are 100 μm. For quantifications, the positive stained area was counted and calculated as percentage of whole tumor section. Values are displayed as mean ± SEM.

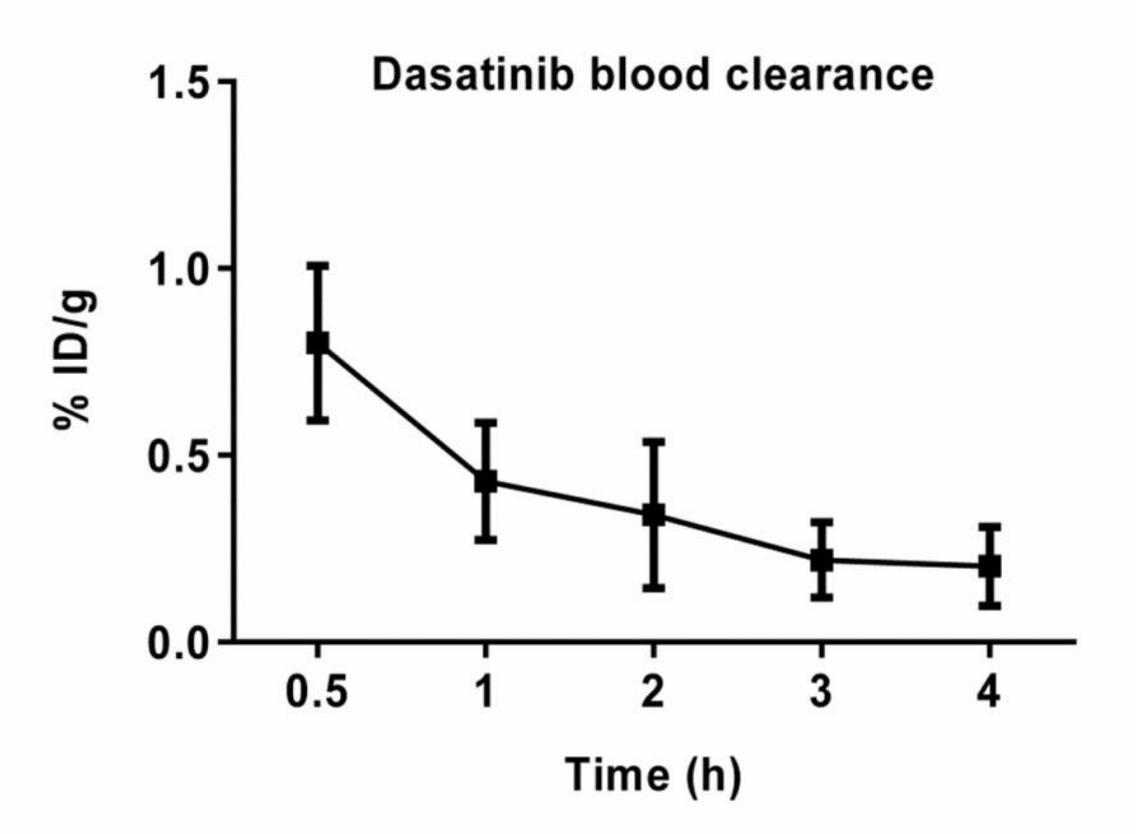

Supplemental Figure 7. Blood clearance of ^{14}C-dasatinib in naïve Ntva mice (n = 4). The blood activity of ^{14}C-dasatinib in Ntva mice is <1% after 30 min. Values are mean ± SE of all mice for each time point.

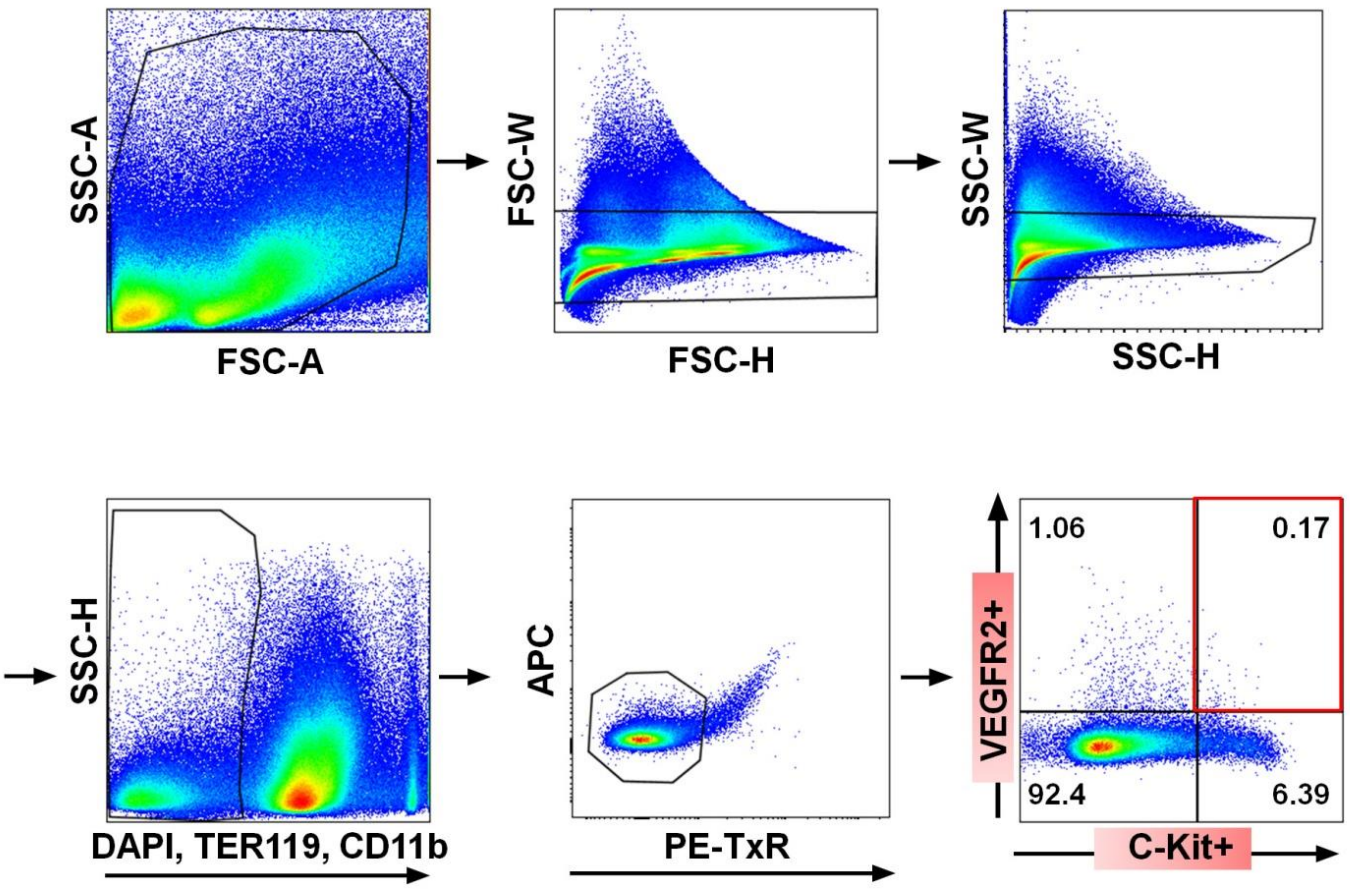

Supplemental Figure 8. Complete flow cytometry gating scheme for the identification of bone marrow EPCs in Ntva mice. After gating out debris in forward versus side scatter (SSC-A versus FSC-A), cell doublets were excluded twice in forward scatter (FSC-W versus FSC-H) and subsequently in the side scatter (SSC-W versus SSC-H). In the next step, cells that stained positive for Pacific blue-Ter119 (red blood cells) or for Pacific blue-CD11b (lineage marker) and dead cells ($DAPI^+$) were excluded. In an additional gating step, a measurement artifact was removed by gating out cells appearing positive for PE Texas red versus APC. The percentage of EPCs was determined in the quadrant 2 as $cKit^+$ and $VEGFR2^+$.

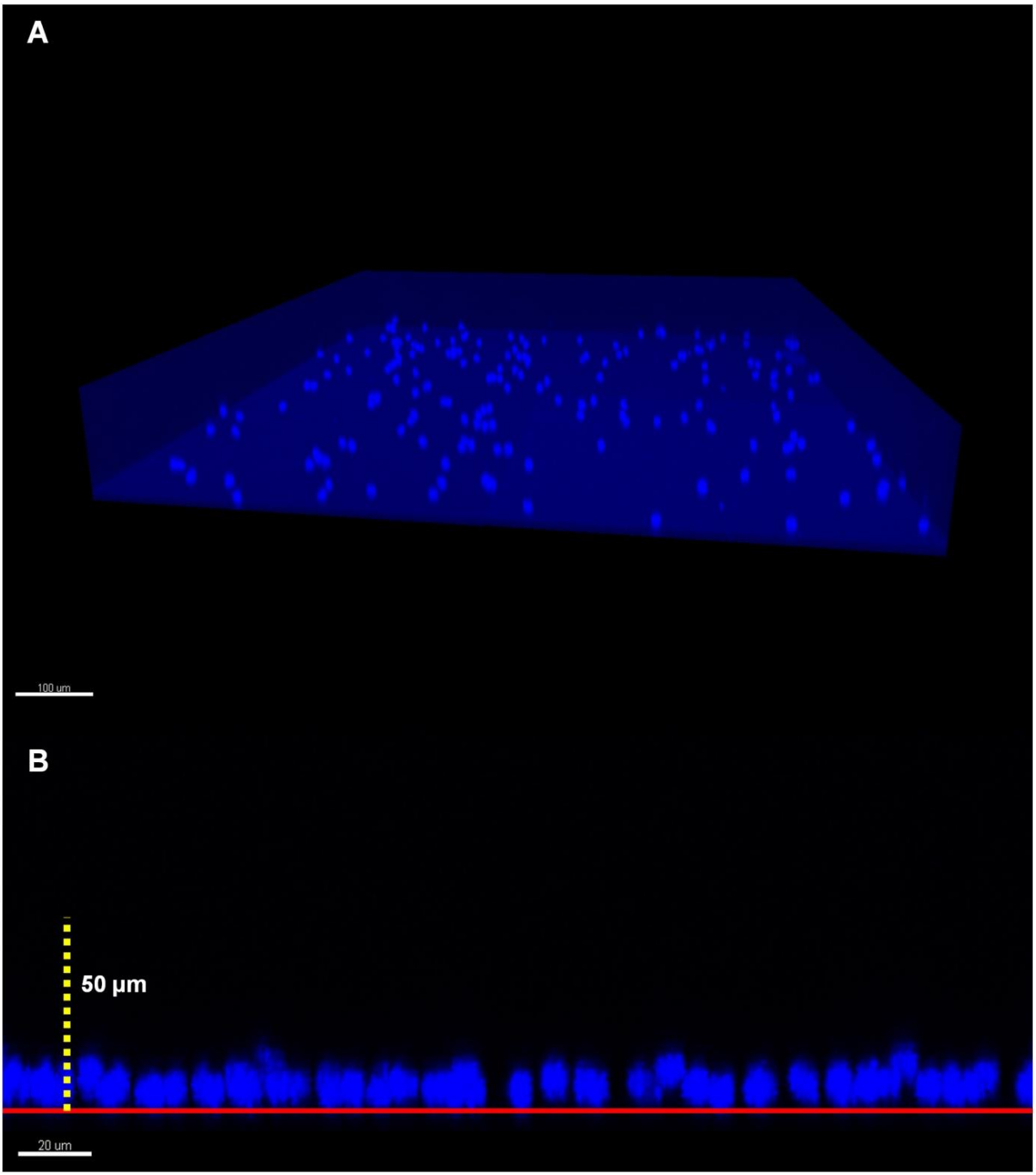

Supplemental Figure 9. Confocal microscopic image of dissociated neurosphere-derived cells that were fixed and stained with DAPI and then placed into an α-particle irradiator dish at a concentration of 344 cells/mm^2. (**A**) 3-dimensional z-stacked image showing the cell distribution in an imaged volume of 0.057 mm^3 (scale bar is 0.100 mm). (**B**) 2-dimensional view illustrating the nuclear (blue DAPI) diameters, geometry (the Mylar boundary is indicated in red), and the approximate path length of the α-particle tracks (indicated with a dashed yellow line). The scale bar is 20 µm.

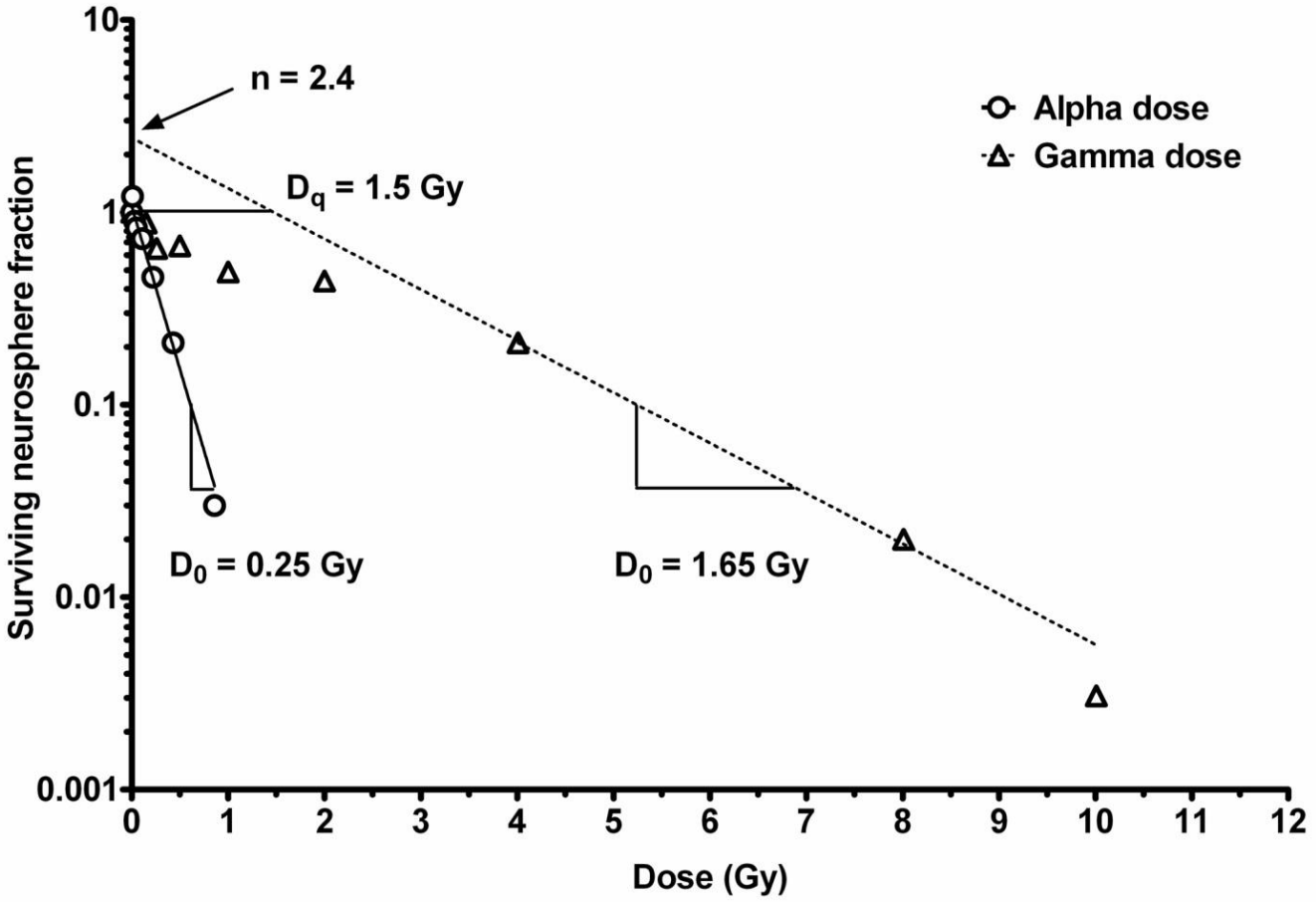

Supplemental Figure 10. Plots of the surviving fraction of neurospheres versus dose for cells that were exposed to varying doses of α-particle and γ-irradiation. The α-particle irradiator exposure time to yield 1 nuclear hit was 23.16 seconds, and 1 Gy (α) resulted from 8 nuclear α-particle hits. α-particle–irradiated cells had a mean lethal dose $D_0(\alpha)$ of 0.25 Gy (2 nuclear hits) and no shoulder was evident in the plot of surviving fraction versus dose, indicating the radiosensitivity of the dissociated cells to α-irradiation and the absence of DNA repair. The γ-irradiated cells had a $D_0(\gamma)$ value of 1.65 Gy, indicating the relative radiation resistance of the same cells to this treatment. In addition, the graphically observed shoulder in the γ-irradiated cell plot indicated a quasi-threshold dose D_q value of 1.5 Gy and an extrapolation number of $n = 2.4$. These two values (D_q and n) relate to the curve's shoulder and indicated the involvement of DNA repair following γ-irradiation. The relative biological effect following α-irradiation, RBEα, was determined by the ratio $D_0(\gamma)/D_0(\alpha)$ and was 6.6.